Host ER–parasitophorous vacuole interaction provides a route of entry for antigen cross-presentation in *Toxoplasma gondii*–infected dendritic cells

Romina S. Goldszmid,[1] Isabelle Coppens,[3] Avital Lev,[2] Pat Caspar,[1] Ira Mellman,[4] and Alan Sher[1]

[1]Immunobiology Section, Laboratory of Parasitic Diseases and [2]Laboratory of Viral Diseases, National Institute of Allergy and Infectious Diseases, National Institutes of Health, Bethesda, MD 20892
[3]Department of Molecular Microbiology and Immunology, Johns Hopkins University Bloomberg School of Public Health, Baltimore, MD 21205
[4]Genentech, Inc., South San Francisco, CA 94080

Toxoplasma gondii **tachyzoites infect host cells by an active invasion process leading to the formation of a specialized compartment, the parasitophorous vacuole (PV). PVs resist fusion with host cell endosomes and lysosomes and are thus distinct from phagosomes. Because the parasite remains sequestered within the PV, it is unclear how *T. gondii*–derived antigens (Ag's) access the major histocompatibility complex (MHC) class I pathway for presentation to CD8$^+$ T cells. We demonstrate that recruitment of host endoplasmic reticulum (hER) to the PV in *T. gondii*–infected dendritic cells (DCs) directly correlates with cross-priming of CD8$^+$ T cells. Furthermore, we document by immunoelectron microscopy the transfer of hER components into the PV, a process indicative of direct fusion between the two compartments. In strong contrast, no association between hER and phagosomes or Ag presentation activity was observed in DCs containing phagocytosed live or dead parasites. Importantly, cross-presentation of parasite-derived Ag in actively infected cells was blocked when hER retrotranslocation was inhibited, indicating that the hER serves as a conduit for the transport of Ag between the PV and host cytosol. Collectively, these findings demonstrate that pathogen-driven hER–PV interaction can serve as an important mechanism for Ag entry into the MHC class I pathway and CD8$^+$ T cell cross-priming.**

CORRESPONDENCE
Romina S. Goldszmid:
rgoldszmid@niaid.nih.gov
OR
Alan Sher:
asher@niaid.nih.gov

Abbreviations used: 4-p-BPB, 4-p-bromophenacyl bromide; Ag, antigen; BMDC, bone marrow–derived DC; CytD, cytochalasin D; ER, endoplasmic reticulum; ERAD, hER-associated degradation system; ExoA, exotoxin A; G6Pase, glucose 6-phosphatase; hER, host ER; HK, heat killed; irr, irradiated; MOI, multiplicity of infection; ova-LB, OVA-coated latex beads; PM plasma membrane; PV, parasitophorous vacuole; PVM, PV membrane; rVV-OVA, recombinant vaccinia viruses expressing OVA; STAg, soluble tachyzoite Ag; TAP, transporter associated with Ag processing; TEM, transmission electron microscopy; TgHK, HK *T. gondii*; Tgirr, irr *T. gondii*; TgOVA, OVA-expressing *T. gondii*.

DCs are specialized antigen (Ag)-presenting cells adept at loading peptides derived from exogenous proteins onto both MHC class I and II molecules (1). Although MHC class II loading occurs entirely within endosomes or lysosomes, the mechanism of cross-presentation on MHC class I is poorly understood (2). Protein Ag's are thought to exit endocytic compartments and reach the cytosol for proteasomal processing. The resulting peptides are then translocated by the transporter associated with Ag processing (TAP) 1/TAP2 into the endoplasmic reticulum (ER; or possibly endosomes) for loading onto MHC class I (2, 3). The pathway of Ag presentation is particularly unclear for intracellular pathogens that dwell in vacuoles sequestered from the cytosol. An important example is provided by *Toxoplasma gondii*, an apicomplexan parasite that resides within a highly specialized parasitophorous vacuole (PV), which is known not to participate in endocytosis or recycling (4, 5). Nevertheless, *T. gondii* mounts strong protective CD8$^+$ T cell responses required for persistent host infection (6, 7).

Tachyzoite-stage parasites infect host cells by an active process that involves the sequential discharge of secretory organelles (micronemes, rhoptries, and dense granules), leading to the formation of a replication-permissive PV (4). Micronemal proteins secreted during the initial steps of invasion facilitate attachment to host cells, and this is followed by the discharge of rhoptries into the cytosol and the evolving PV.

The Rockefeller University Press $30.00
J. Exp. Med. Vol. 206 No. 2 399-410
www.jem.org/cgi/doi/10.1084/jem.20082108

Proteins derived from dense granules then actively remodel the PV membrane (PVM), in turn rendering the PV incapable of endosome/lysosome fusion (8, 9). At the same time, *T. gondii* modifies the PVM to allow for nutrient acquisition by generating pores that permit free diffusion of small molecules <1.3 kD (10), by recruiting host mitochondria and ER that may serve as a potential source of lipids (11–13) and by scavenging cholesterol from the host endocytic pathway (14).

Although the PVM provides a barrier for intact protein Ag escape, recent studies have indicated that $CD8^+$ T cell priming by *T. gondii*–infected cells requires TAP (15–17) as well as proteasomal processing, but is independent of endosomal pH and protease activity (15), arguing that it involves the cytosolic MHC class I machinery. In this study, we have directly investigated the pathway by which *T. gondii*–derived Ag exits the PV for MHC class I presentation. We demonstrate that this process involves interconnectivity between the host ER (hER) and PV, and the subsequent retrotranslocation of parasite molecules into the host cell cytoplasm. In marked contrast, internalization of live or dead *T. gondii* into conventional phagosomes that do not fuse with ER fails to facilitate cross-presentation. Our findings thus implicate pathogen-driven recruitment of hER as an important route of entry for exogenous Ag's into the MHC class I pathway for *T. gondii* and, possibly, other vacuole-dwelling microbes.

RESULTS

$CD8^+$ T cell priming requires active infection

Previous work suggested that *T. gondii*–derived Ag's access the host cell cytosol and there intersect the MHC class I pathway for cross-presentation (15–17). This could reflect the phagocytosis of infected cells or dead parasites by professional Ag-presenting cells (e.g., DCs) or the direct infection of DCs. Because a system to detect natural *T. gondii* $CD8^+$ and $CD4^+$ T cell epitopes in common haplotypes was unavailable, we used as a model transgenic parasites expressing a truncated form of OVA, secreted via dense granules that release their contents inside the PV (Fig. S1, available at http://www.jem.org/cgi/content/full/jem.20082108/DC1), to track Ag-specific T cell responses to the parasite.

To determine whether active infection of DCs is required for $CD8^+$ T cell priming in vivo, B6.SLJ congenic mice that had received purified CFSE-labeled naive transgenic OT-I $CD8^+$ T cells specific for the OVA-derived peptide SIINFEKL were subsequently injected with live, live irradiated (irr), or paraformaldehyde-killed (fix) OVA-expressing *T. gondii* (TgOVA), TgOVA-infected MHC class I–deficient ($MHC\text{-}I^{-/-}$) DCs, or the nontransgenic parental RH parasite strain. Draining lymph nodes were harvested 3 d after challenge and OT-I $CD8^+$ T cell proliferation was measured. The transferred cells were found to proliferate only in those mice that were challenged with live TgOVA or irr TgOVA (TgOVAirr) parasites (Fig. 1 A). This T cell priming was not caused by the increased Ag load resulting from parasite replication, as nonmultiplying irr tachyzoites, which also form a PV, induced the same level of T cell activation. As an additional positive control, we showed that OT-I $CD8^+$ T cell proliferation is also observed in mice that received TgOVA-infected WT DCs (Fig. S2 A, available at http://www.jem.org/cgi/content/full/jem.20082108/DC1). Because $MHC\text{-}I^{-/-}$ DCs that are as efficiently infected as their WT counterparts (Fig. S2 B) cannot directly present Ag to $CD8^+$ T lymphocytes, these data support previous in vitro studies (18) indicating that direct infection rather than uptake of dead parasites or bystander infected cells is required for cross-presentation of *T. gondii*–derived OVA. Similarly, only actively infected DCs stimulated IFN-γ production from polyclonal $CD8^+$ T cells derived from nontransgenic mice infected with an avirulent strain of *T. gondii* (ME-49; Fig. 1 B), suggesting that active infection is also required for cross-presentation of natural parasite Ag.

To elucidate the mechanism by which Ag from live *T. gondii* access the MHC class I pathway, we turned to an in vitro system in which bone marrow–derived DCs (BMDCs) were exposed to infective TgOVAirr or noninfective heat-killed (HK) TgOVA (TgOVAHK) tachyzoites or nontransgenic parasites. After fixation, the parasite-exposed DCs were co-cultured with CFSE-labeled naive OT-I cells, and T cell proliferation was measured as a readout of Ag processing and presentation. In agreement with the in vivo data, DCs that were actively infected induced strong $CD8^+$ T cell proliferation (Fig. 1 C). Although DCs that had phagocytosed dead parasites efficiently processed and presented parasite-derived OVA peptide to naive transgenic OT-II $CD4^+$ T cells, they were unable to cross-present parasite-derived SIINFEKL peptide to $CD8^+$ T cells (Fig. 1, C and D). A similar lack of response was observed when splenic-derived DCs were substituted for BMDCs (Fig. S3, available at http://www.jem.org/cgi/content/full/jem.20082108/DC1).

The inability of DCs to cross-present phagocytosed parasites led us to ask if dead tachyzoites could exert an inhibitory effect in trans that would block cross-presentation of Ag derived from live parasites. DCs were incubated with a mixture of TgOVAirr and HK *T. gondii* (TgHK), or TgOVAHK and irr *T. gondii* (Tgirr) tachyzoites. Although the majority of the infected DCs also contained phagocytosed parasites (Fig. S4, available at http://www.jem.org/cgi/content/full/jem.20082108/DC1), proliferation of naive OT-I cells was observed only with DCs in which OVA was expressed by irr tachyzoites (Fig. 1 E), thus indicating that phagocytosis of dead parasites does not inhibit cross-presentation of vacuole-derived Ag, nor does active infection promote presentation of Ag derived from tachyzoites within phagosomes. In parallel experiments, uptake of dead *T. gondii* parasites failed to inhibit cross-presentation of Ag from phagosomes containing OVA-coated latex beads (ova-LB; Fig. 1 F and Fig. S4 B), confirming that phagocytosed tachyzoites do not have a generalized suppressive effect on MHC class I presentation.

Blocking parasite invasion inhibits cross-presentation

Because dead parasites were not cross-presented to OT-I T cells, we next asked if phagocytosis of live tachyzoites can lead to $CD8^+$ T cell priming. Live TgOVA parasites were

pretreated with 4-p-bromophenacyl bromide (4-p-BPB), an irreversible inhibitor of phospholipase A_2 that completely blocks the host cell invasion process without metabolically disabling the parasite (19). 4-p-BPB suppressed parasite invasion in a dose-dependent fashion and, in a quantitatively similar manner, inhibited cross-presentation to OT-I T cells (Fig. 2, A and B). Nevertheless, 4-p-BPB–treated parasites were clearly phagocytosed and targeted to LAMP1$^+$ compartments (Fig. 2 C and not depicted) and, as expected, efficiently presented to CD4$^+$ OT-II cells (Fig. 2 D). As a control, it was shown that 4-p-BPB–treated tachyzoites secreted similar amounts of OVA as their untreated counterparts (Fig. S5, available at http://www.jem.org/cgi/content/full/jem.20082108/DC1). Thus, phagocytosis fails to lead to CD8$^+$ T cell priming even after uptake of live parasites. Similarly, treatment with cytochalasin D (CytD), which blocks tachyzoite invasion without inhibiting discharge of the rhoptry secretory organelles (20, 21), also prevented Ag cross-presentation (Fig. 2, E and F). The latter observation argues against a role for direct injection of parasite-derived Ag into the cytosolic MHC class I presentation pathway.

Antibody-opsonized tachyzoites are avidly ingested and, in common with conventional phagocytic cargo, are delivered to phagolysosomes (8, 9). In other systems, uptake of Ag through FcγR ligation is known to promote cross-presentation by DCs (22). However, targeting of either live (4-p-BPB–treated) or dead parasites to FcγR by means of antibody opsonization failed to result in MHC class I cross-presentation while efficiently priming MHC class II–dependent OT-II T cell proliferation (Fig. S5). Again, this was shown not to be caused by an effect of opsonization on OVA secretion by the parasites (Fig. S5).

Evidence for fusion between hER and PV during active infection of DCs

Recruitment of ER components into Ag containing endo-/phagocytic organelles has been proposed as a mechanism to explain cross-presentation in other systems (23–25). Live *T. gondii*

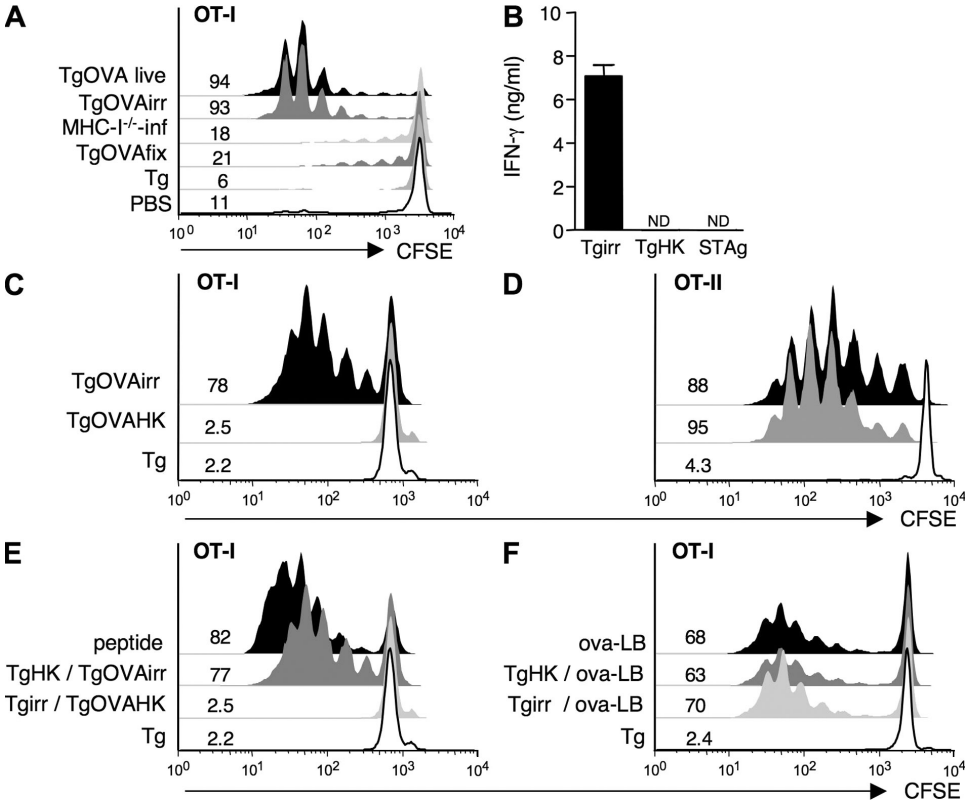

Figure 1. Only actively infected DCs cross-present *T. gondii*–derived Ag to CD8$^+$ T cells. (A) CFSE-labeled naive OT-I CD8$^+$ T cells were transferred into congenic recipients, which were subsequently challenged with either live, live irr, or noninfective killed (fix) TgOVA, TgOVA–infected MHC-I$^{-/-}$ DCs (MHC-I$^{-/-}$ inf), nontransgenic parasites (Tg), or PBS. Proliferation of OT-I cells was measured 3 d later in the draining lymph nodes. (B) Purified CD8$^+$ T cells from infected C57BL/6 mice were restimulated with DCs exposed to live Tgirr or TgHK tachyzoites, or to soluble parasite extract (STAg), and IFN-γ production was measured by ELISA in 48-h supernatants. The values shown are the means ± SD of the ELISA readings from three mice per group. No cytokine production was detected when T cells were stimulated with DCs alone. (C and D) CFSE-labeled OT-I (C) or OT-II (D) cells were incubated with DCs preexposed to TgOVAirr, TgOVAHK, or Tg tachyzoites. (E and F) DCs were incubated with a mixture of TgHK and TgOVAirr tachyzoites (TgHK/TgOVAirr), Tgirr and TgOVAHK (Tgirr/TgOVAHK), or Tg alone, or were pulsed with SIINFEKL peptide (E) or ova-LB alone or mixed with either TgHK (TgHK/ova-LB) or Tgirr (Tgirr/ova-LB; F), and were cultured with CFSE-labeled OT-I T cells. In C–F, T cell proliferation was measured on day 3. The data shown in A–F are representative of at least three experiments. The numbers to the left of each histogram represent the percentage of cells showing reduced CFSE content as a measure of proliferation.

is known to recruit hER in proximity to PV as a potential source of lipids in fibroblasts and macrophages (11, 26), although direct fusion between hER and PVM has never been documented. Immunofluorescence microscopy performed on actively infected DCs revealed that a luminal ER marker (KDEL-modified proteins) exhibited a circumferential staining pattern colocalizing with the PVM protein GRA7, indicating that these two compartments are in close apposition, which would allow for possible fusion events. (Fig. 3 A). A similar staining pattern was observed when antibodies against the ER markers Sec61 (Fig. 3 B), calnexin, and calreticulin were used (not depicted). The occurrence of fusion events was directly demonstrated by immunogold labeling, which showed that gold particles detecting KDEL proteins localized to the PV lumen, between the parasite plasma membrane (PM) and the PVM (Fig. 3 C). In contrast, no delivery of hER contents to the phagosomal lumen was detected in phagosomes after ingestion of opsonized live or dead parasites (Fig. 3 D). Consistent with previous findings, PVM fusion with host lysosomes was not observed in infected cells, whereas lysosomal fusion was clearly evident in *T. gondii*–containing phagosomes (Fig. S6, available at http://www.jem.org/cgi/content/full/jem.20082108/DC1) (8, 9). In the described experiments using anti-KDEL antibodies, only background staining of tachyzoites within vacuoles was seen, arguing against the possibility that the proteins detected were of parasite origin.

To further confirm the presence of hER luminal components within the PV lumen in infected cells, we used in situ immunocytochemical staining for the ER-specific marker glucose 6-phosphatase (G6Pase), an enzyme absent in *T. gondii* (27, 28). Electron dense reaction product was readily detected in the lumen of hER and nuclear envelope (Fig. 4 A). Importantly, substantial amounts of reaction product were detected within the PV lumen itself (Fig. 4, A–D). Staining of the PVM itself was also routinely visualized (Fig. 4, C and D), further demonstrating direct transfer of hER components into the PV. No reaction product was observed within the parasite, ruling out the possible nonspecific contribution of *T. gondii*–derived nucleoside triphosphatases or other phosphatases to the staining patterns observed. These results were quantified, confirming that hER–PV fusion occurred in a majority of cases after the entry of live parasites (Fig. 5 A). In marked contrast to the findings with live or irr tachyzoites (Fig. 4 and Fig. 5 B), no reaction products were detected in parasite-containing phagosomes (Fig. 5, C and D), consistent with the absence of associated hER as determined by direct immunogold labeling (Fig. 3 D). Collectively, these observations indicated that the hER luminal content can be discharged into the PV, thereby revealing direct communication between these two compartments.

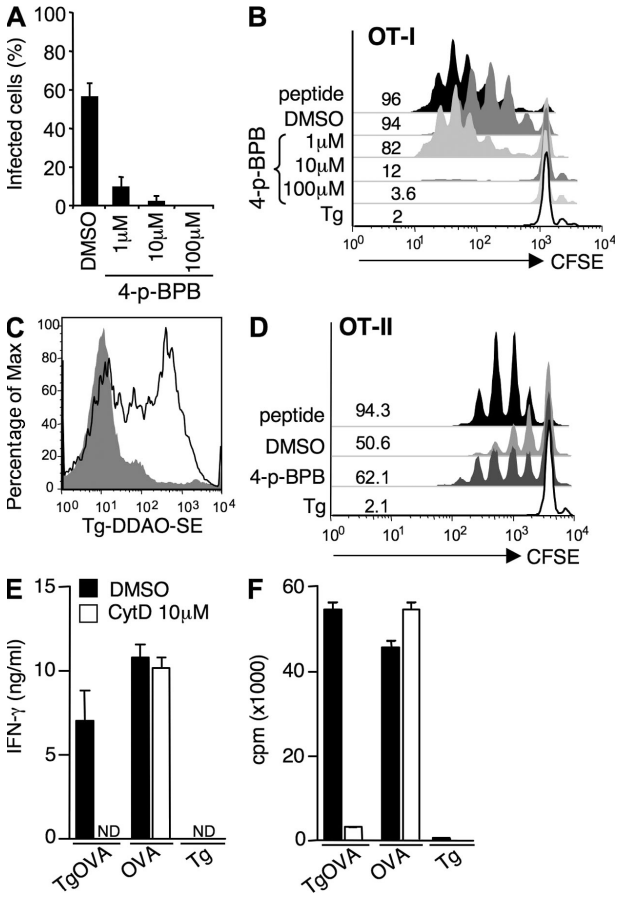

Figure 2. Blocking different steps of the invasion process inhibits cross-presentation. (A–D) TgOVA parasites were pretreated with 4-p-BPB or the DMSO vehicle alone and were incubated with DCs. (A) Effect of 4-p-BPB treatment on parasite invasion as determined by the percentage of infected cells. (B) Effect of parasite 4-p-BPB treatment on T cell activation. CFSE-labeled OT-I cells were incubated with the same DCs as described in A, DCs infected with Tg or DCs pulsed with SIINFEKL peptide. (C) DDAO-SE–labeled 4-p-BPB–treated tachyzoites were incubated with DCs at 37°C (open histogram) or 4°C (shaded histogram), and parasite uptake was assessed by flow cytometry at 2.5 h. The histograms shown are gated on $CD11c^+$ cells. (D) CFSE-labeled OT-II cells were incubated with DCs preexposed to 100 μM 4-p-BPB or DMSO-treated TgOVA, Tg parasites, or were pulsed with peptide. In B and D, T cell proliferation was measured on day 3. The numbers to the left of each histogram represent the percentage of cells showing reduced CFSE content as a measure of proliferation. (E and F) DCs were incubated with Tg or TgOVA parasites in the presence or absence of CytD for 30 min, washed, and incubated for an additional 3.5 h before fixation. Microscopic examination revealed that CytD treatment completely inhibited cell invasion (not depicted). In another set of samples, CytD-pretreated or untreated DCs were incubated with 1 mg/ml of soluble OVA for the same time period and fixed. OT-I T cells were then added to the DC cultures, and IFN-γ production (E) and thymidine incorporation (F) were measured at 48 and 72 h, respectively. The values shown are means ± SD of triplicate cultures. The data presented in A–F are representative of three experiments performed. ND, not detected.

Cross-presentation requires ER retrotranslocation

The direct correlation of hER–PV fusion with Ag cross-presentation suggested that *T. gondii* might exploit the hER-associated degradation system (ERAD) to transport proteins from the PV into the cytosol. Exotoxin A (ExoA) from *Pseudomonas aeruginosa* has previously been shown to block the ERAD translocon subunit sec61 (29). ExoA treatment was found to markedly inhibit activation of naive OT-I $CD8^+$

T cells by TgOVA-infected DCs while not affecting the presentation of exogenously added peptide (Fig. 6, A and B). Importantly, ExoA treatment had no effect on the presentation of endogenously generated SIINFEKL when DCs were infected with recombinant vaccinia viruses expressing OVA (rVV-OVA; Fig. 6, C and D). ExoA treatment of parasite-infected DCs also resulted in decreased expression of cell-surface MHC class I (K^b)–SIINFEKL complexes, as detected by staining with the 25.D1.16 specific antibody, thus confirming that the observed effects on T cell activation are caused by a lack of OVA cross-presentation (Fig. 6 E). In contrast, ExoA treatment had no effect on surface expression of MHC class I in parasite-infected DCs or MHC class I–peptide complexes in rVV-OVA–infected or peptide-pulsed DCs (Fig. S7, A–C, available at http://www.jem.org/cgi/content/full/jem.20082108/DC1). Similarly, ExoA treatment failed to affect tachyzoite invasion or parasite protein secretion (Fig. S7, D and E). These findings argued that hER retrotranslocation plays a major role in the cross-presentation of *T. gondii*–derived proteins during active infection of DCs.

DISCUSSION

In essentially every case studied, vacuole-dwelling pathogens trigger $CD8^+$ T cell responses despite their sequestration from the cytosolic MHC class I presentation pathway (30–32). *T. gondii* provides a powerful model for dissecting the cellular basis of this poorly understood mechanism in the host response to microbes. Of particular note is the striking dependence, both in vitro and in vivo, of MHC class I presentation on active *T. gondii* infection and the inability of DCs to cross-present phagocytosed live or dead parasites or infected cells. Our findings indicate that the PV, in contrast to the phagosome, facilitates entry of *T. gondii* Ag into the class I pathway and further argue that the ability of parasite-containing PV to

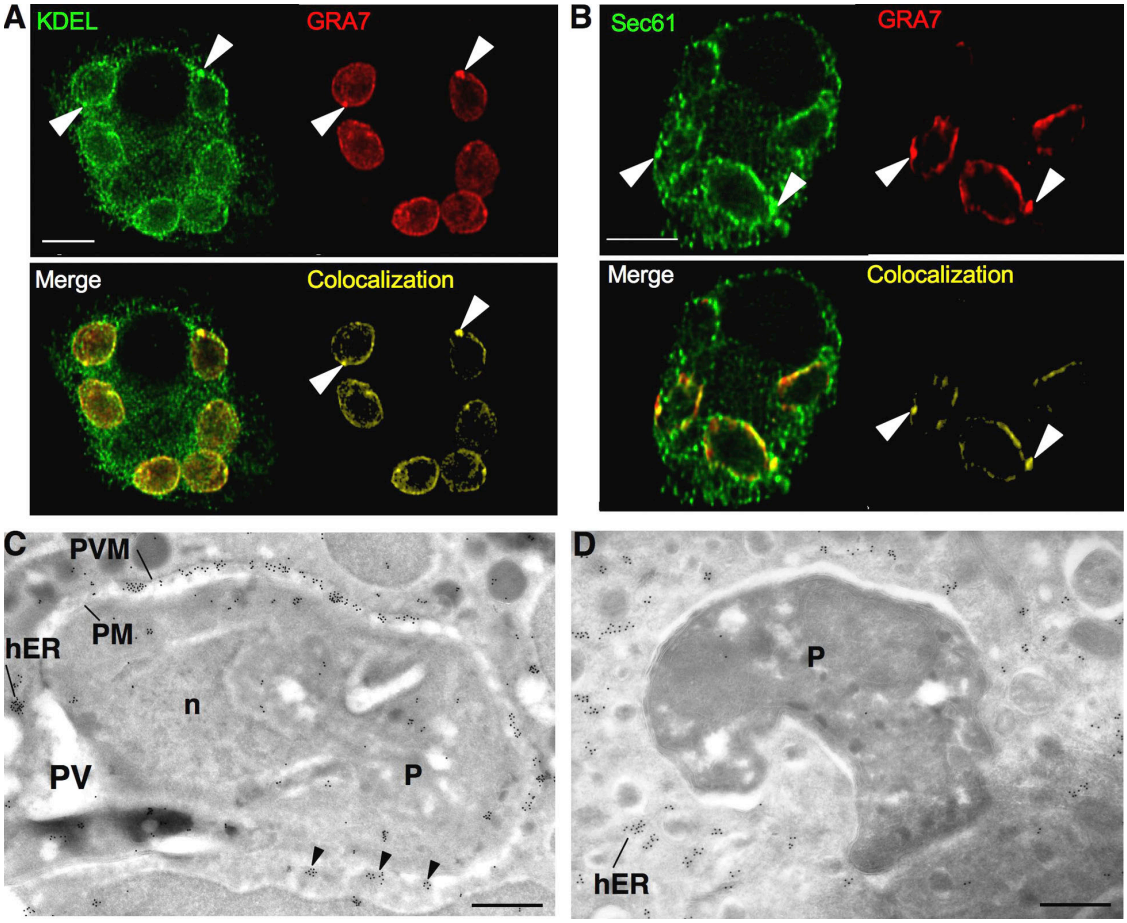

Figure 3. Association and fusion of hER with PV containing live *T. gondii* but not with phagosomes containing HK tachyzoites. (A and B) Confocal microscopy of DCs incubated with live *T. gondii* tachyzoites and stained with a combination of anti-KDEL (green; A) or anti-Sec61 (green; B) and anti-GRA7 (a parasite-dense granule protein localized at the PVM; red). The cells were examined by confocal microscopy, and the images were deconvolved and colocalization analysis was performed (yellow). Multiple PVs can be seen within the cell, and arrowheads pinpoint specific areas of intense colocalization of KDEL (A) or Sec61 (B) with PVM-associated GRA7. (C and D) Immuno-EM performed on cryosections of DCs showing (C) a live parasite inside a PV where hER components are detected between the PVM and parasite PM (arrowheads) revealed by anti-KDEL antibodies, or (D) a DC that has phagocytosed a noninfective parasite and where no hER is evident surrounding the parasite-containing phagosome. The images shown are representative of at least three experiments performed. n, nucleus; P, parasite. Bars: (A and B) 5 µm; (C and D) 0.2 µm.

recruit and physically interact with hER is intimately associated with the process of cross-presentation.

In addition to its involvement here, retrotranslocation has also been implicated as an important step in the cross-presentation of both soluble and particulate-bound Ag (23, 24, 33). In the latter situation, ER-phagosome fusion has been proposed in several studies as a mechanism by which exogenous Ag exits from the phagosomal vacuole (23, 24), although the

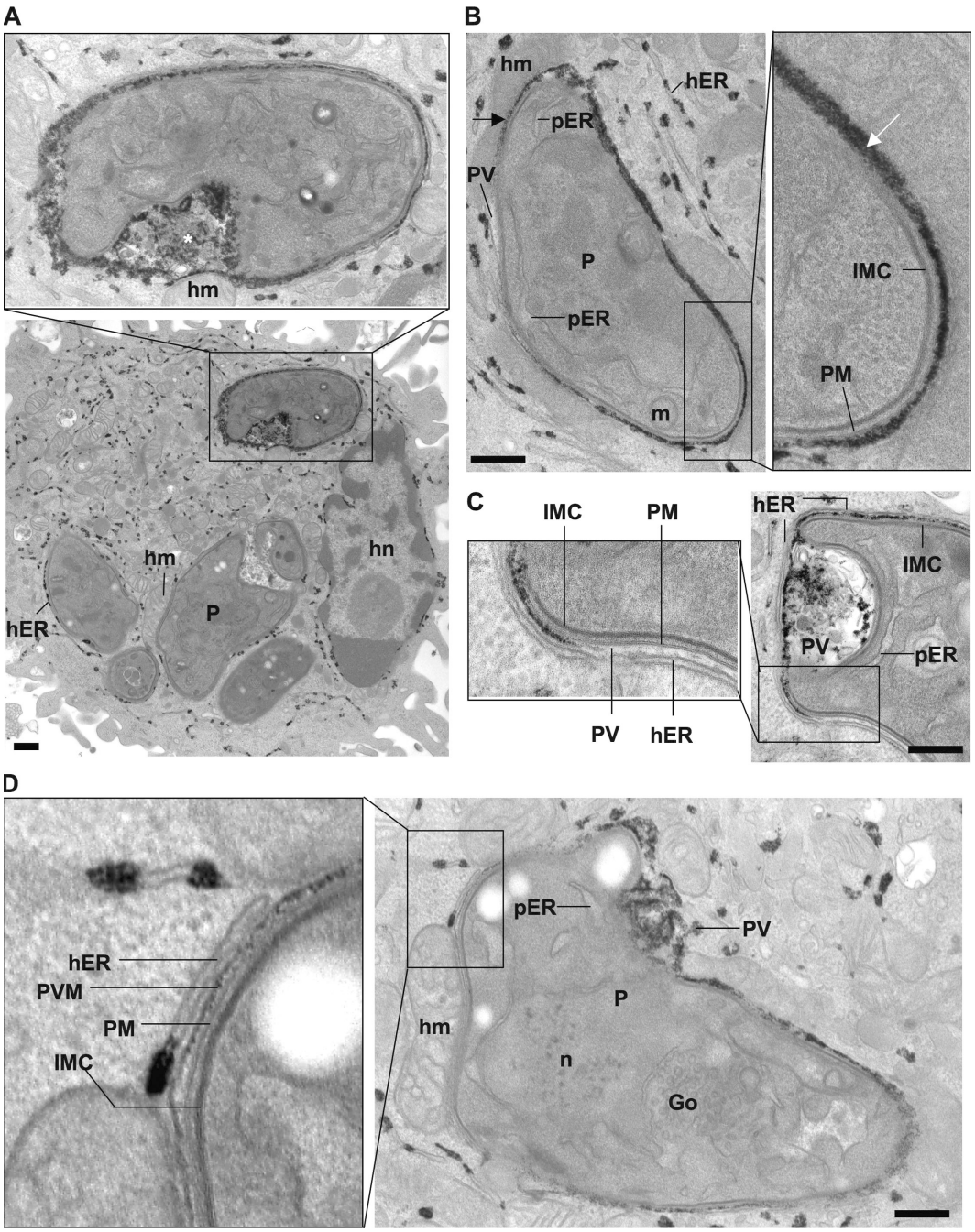

Figure 4. Localization of G6Pase activity in DCs infected with live *T. gondii*. (A–D) TEM of *T. gondii*–infected DCs. (A) Infected DCs showing dotted G6Pase activity staining around most of the PVs, indicating the presence of associated hER. The inset shows an example of a PV in which a more diffuse continuous staining is evident on the PVM and/or PV content. The asterisk designates PV lumen. (B–D) PV displaying strong G6Pase activity adjacent to the parasite PM in the vacuolar space. (B) The black arrow indicates an example of staining localized in the region between a host mitochondrion and the parasite suggestive of PV lumen localization. The white arrow in the inset illustrates the diffuse staining seen around the parasite that contrasts with the dotted staining of hER. (C and D) PV detail showing staining in the vacuolar space (C, inset) and associated with PVM facing the hER (D, inset). Parasite ER shows no labeling on all sections analyzed, confirming the absence of G6Pase homologue. The images shown are representative of at least 150 PVs examined. Go, Golgi; hm, host mitochondrion; IMC, inner membrane complex; m, mitochondrion; n, nucleus; P, parasite; pER, parasite ER. Bars, 0.5 µm.

physiological relevance of these findings has been contested (34). It is of particular interest, then, that in the case of *T. gondii*–infected DCs, parasite-containing phagosomes fail to recruit or fuse with the ER, nor do they permit the transit of Ag into the cytosolic MHC class I pathway. Instead, active remodeling of the PV by the parasite is required for both processes, arguing that for intracellular pathogens, cross-presentation requires more than simple delivery of live or dead organisms into a phagosome. The ability of phagosomes to cross-present Ag derived from protein-coated beads (Fig. 1 F) (23, 24), although seemingly contradictory, may simply reflect the distinct nature of the phagosomal cargo and perhaps the levels of Ag available for presentation.

In this paper, we argue, based on the observation of molecular exchange between hER and PV, that direct fusion of

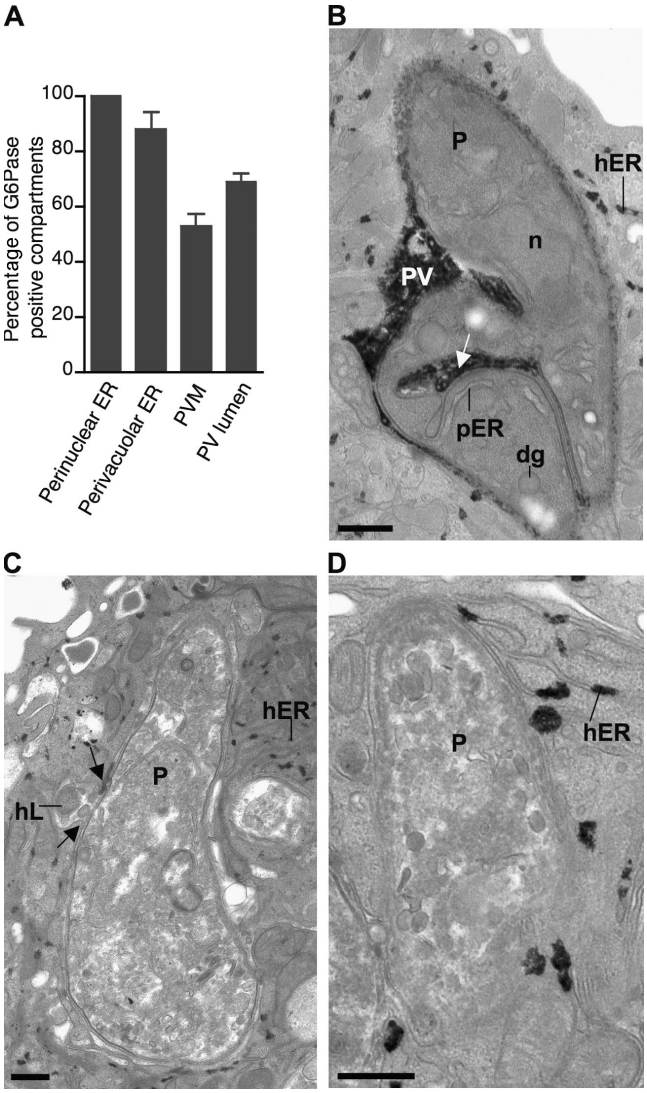

Figure 5. Quantification of G6Pase activity in infected DCs and absence of staining in DCs containing HK or opsonized *T. gondii* tachyzoites. (A) Quantification of G6Pase-positive compartments in a single EM plane in actively infected DCs. The data show the mean percentages ± SD of the compartments stained in each category for a total of 60 PVs examined. (B–D) TEM showing (B) a PV containing an irr parasite, and a phagosome containing (C) an antibody-opsonized or (D) an HK parasite. Note the absence of G6Pase staining in the phagosomal lumen (C and D) in contrast to the vacuolar space (B). Arrows in C show fusion of a host lysosome (hL) with the opsonized parasite-containing phagosome. dg, dense granule; n, nucleus; pER, parasite ER. Bars, 0.5 µm.

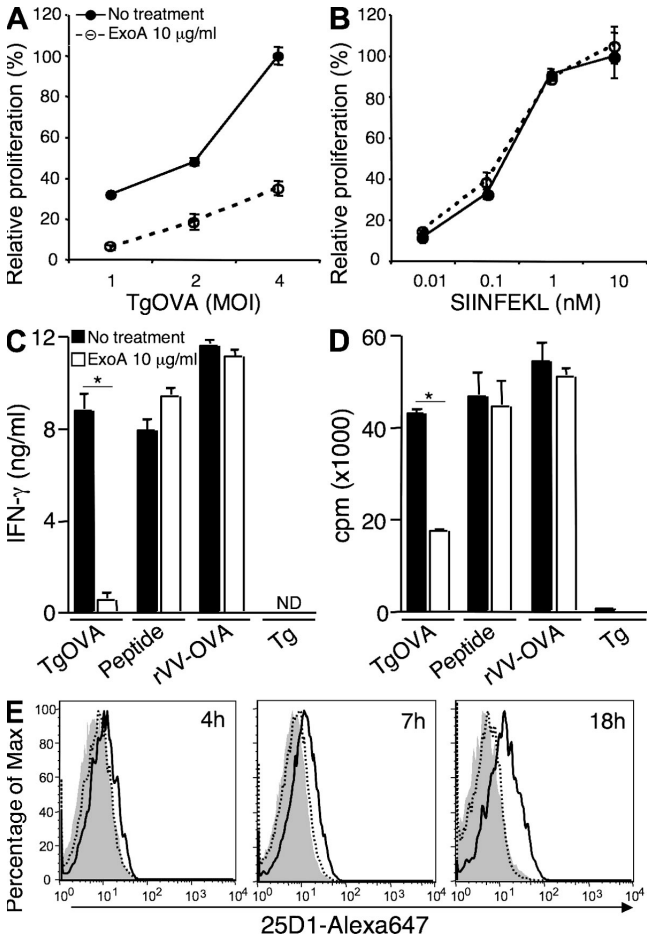

Figure 6. ExoA inhibits cross-presentation of *T. gondii*–derived Ag. (A and B) DCs were incubated with different MOIs of TgOVA parasites or increasing concentrations of SIINFEKL peptide in the presence or absence of ExoA and were fixed before co-culture with OT-I cells. T cell proliferation was measured at 72 h by thymidine incorporation. The values indicate the means ± SD of triplicate cultures. (C and D) DCs were incubated with TgOVA parasites (MOI = 4), SIINFEKL peptide, rVV-OVA, or Tg tachyzoites for 3.5 h in the presence or absence of ExoA and were fixed before co-culture with OT-I cells. (C) IFN-γ production and (D) thymidine incorporation were measured at 48 and 72 h, respectively. The values shown are means ± SD of triplicate cultures. Data pairs indicated by asterisks represent significant differences between conditions ($P < 0.001$). (E) DCs were incubated with TgOVA-YFP parasites in the presence or absence of ExoA. Expression of K^b–SIINFEKL complexes on the cell surface was assessed at different time points after infection by staining with the 25D1.16 mAb, followed by flow cytometry gating on $CD11c^+YFP^+$ (infected) or YFP^- (uninfected) cells. Shaded histograms indicate uninfected cells, continuous line histograms indicate infected cells without treatment, and dotted line histograms indicate infected cells treated with ExoA. Data shown in A–E are representative of at least three experiments. ND, not detected.

these two compartments is a major route of Ag export into the cytosol. Because no defined channels or breaches could be detected at the points of hER–PV membrane contact, it is likely that if such structures exist they are spatially restricted or highly transient. Alternatively, it is possible that exchange between the two compartments is mediated by "kiss-and-run"–like events (35) that would allow for transfer of contents between hER and PV with very little or no exchange of membrane constituents, or perhaps by specialized fine membrane extensions analogous to the mitochondria-associated membranes that facilitate communication between ER and mitochondria in mammalian cells and yeast (36, 37). In this regard, we and others have noted vesicle-like structures emanating from the PV that could also serve as an exit route for Ag. Regardless of whether these structures are involved in Ag transport, they too must eventually fuse with hER to allow for the observed requirement for retrotranslocation. Given that both immunogold and immunofluorescence labeling clearly indicate hER membrane components and the PV membrane to be continuous, it appears that the interaction between these two compartments is stable rather than transient and that direct fusion is the more likely explanation for Ag transfer.

The observed requirement for retrotranslocation argues strongly against several alternative mechanisms that might explain cross-presentation in *T. gondii* infection. As noted above, previous work has documented the presence of pores in the PVM that allow the exchange of small molecules between the PV and cytosol. Nevertheless, if direct loading of MHC class I with peptides introduced into the cytoplasm by this route was the major mechanism by which *T. gondii* Ag access the class I pathway, then no requirement for retrotranslocation as well as proteasomal degradation would be expected. Similarly, it has been shown that during the invasion process parasite proteins are injected directly into the cytosol (20, 38–40), thereby providing yet another possible route for entry of *T. gondii* Ag into the class I pathway. However, our finding that Ag cross-presentation is inhibited by CytD argues against such a mechanism, which again also would not necessarily require retrotranslocation. Although recent studies have described autophagy in association with PV disruption and parasite degradation in activated *T. gondii*–infected macrophages (41–43), we have not observed this process in infected DCs, nor is cross-presentation blocked by treatment of the cells with drugs that inhibit autophagy (unpublished data). Therefore, although autophagy may play an important role in parasite clearance, it seems unlikely that the process contributes significantly to cross-presentation of parasite-derived Ag by *T. gondii*–infected DCs.

In summary, we propose that in the situation of *T. gondii*, active infection associated with PV formation results in the establishment of PVM–hER junctions. Ag secreted into the PV gain access to the hER through these junctions, and then retrotranslocate through the ERAD system to enter the cytosol for processing and loading onto MHC class I (Fig. 7). Recent findings demonstrating a role for the ER aminopeptidase associated with Ag processing in the final trimming of

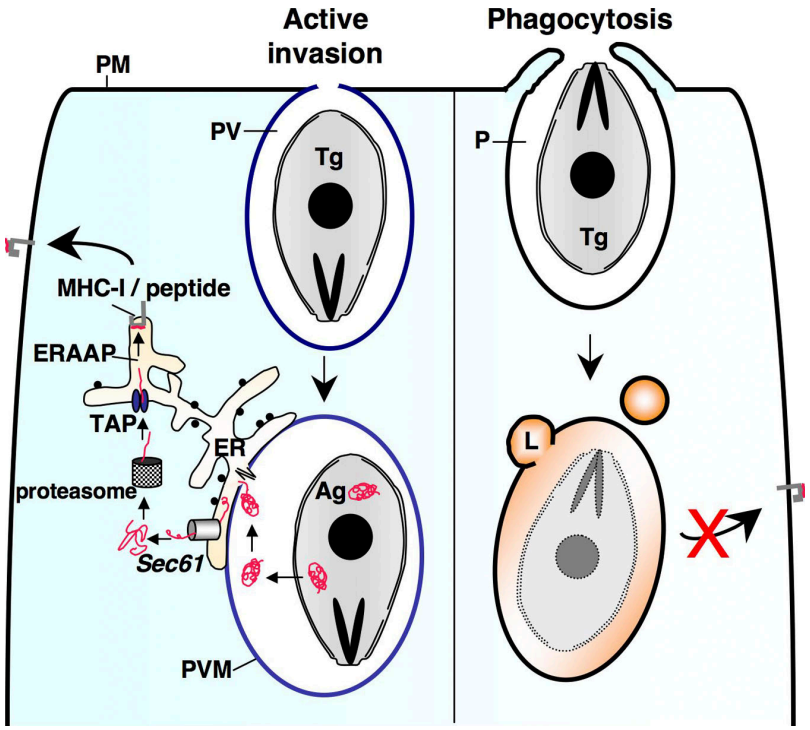

Figure 7. Proposed mechanism for cross-presentation of *T. gondii*–derived Ag. (left) Shown are events occurring after active invasion of DCs by live tachyzoites. (right) No cross-presentation is observed after phagocytic uptake of the parasites. Ag, *T. gondii*–derived Ag; ER, hER; ERAAP, ER aminopeptidase associated with Ag processing; L, lysosome; P, phagosome; Tg, *T. gondii*.

a *T. gondii* GRA6–derived epitope are consistent with such a pathway (44). Although our evidence supports a major role for hER–PV fusion in cross-presentation of *T. gondii*–derived Ag by infected DCs, formal proof of this hypothesis would require selective blockade of hER recruitment to the PV. Unfortunately, there are as yet no inhibitors available that specifically target this process. In addition, it will be important to confirm these findings using the model Ag OVA with studies using naturally occurring parasite epitopes. Several endogenous parasite $CD8^+$ T cell epitopes that were described after the completion of this project are possible candidates for such an analysis (44, 45).

It has been hypothesized that *T. gondii* recruits hER to the PV to provide a mechanism for membrane biogenesis and/or parasite nutrient acquisition (11, 26). It is tempting to speculate that *T. gondii* exploits the same intracellular pathway to present Ag for the induction of $CD8^+$ T cell responses that are critical for promoting pathogen latency and interhost transmission, and thus, for its success as a vertebrate parasite. Further dissection of this highly efficient natural mechanism for the stimulation of $CD8^+$ T cell–dependent immunity may provide important insights applicable to the design of effective vaccines against intracellular pathogens.

MATERIALS AND METHODS

Mice. C57BL/6 mice were purchased from Taconic. β_2-microglobulin–deficient (MHC-$I^{-/-}$), B6.SJL congenic, C57BL/6 OT-I/RAG1, and OT-II TCR transgenic mice were provided by Taconic from the National Institute for Allergy and Infectious Diseases (NIAID) animal supply contract. All mice were maintained in an NIAID, National Institutes of Health (NIH) animal care facility under specific pathogen-free conditions and were treated in accordance with the regulations and guidelines of an animal study proposal approved by the Animal Care and Use Committee of the NIH. Age- (6–8 wk) and sex-matched animals were used in all experiments.

Antibodies and reagents. CytD, 4-p-BPB, and ExoA from *P. aeruginosa* were obtained from Sigma-Aldrich, OVA was obtained from Thermo Fisher Scientific, and CFSE and CellTrace Far Red DDAO-SE were purchased from Invitrogen. The antibodies used for flow cytometry included anti-CD8–PerCP, anti-CD4–PE, anti-CD3–allophycocyanin (APC), anti-CD11c–PE, anti–H2-K^b–FITC, and anti-LAMP1 (all from BD), and anti-CD45.1–PE and anti-CD45.2–APC (eBioscience); the mAb specific for K^b–SIINFEKL complex 25D1.16 (46) conjugated with Alexa Fluor 647 was provided by J. Yewdell and J. Bennink (NIAID, NIH, Bethesda, MD). The antibodies used for immunofluorescence and immunogold labeling included rabbit polyclonal anti-OVA (Sigma-Aldrich), anti-KDEL (Assay Designs), anti-Sec61b (Proteintech Group, Inc.), rabbit polyclonal anti-GRA7 (14), and polyclonal anti-SAG1 (provided by M. Grigg, NIAID, NIH, Bethesda, MD). The secondary antibodies were goat anti–rabbit, goat anti–mouse, and anti–rat conjugated with either Alexa Fluor 488 or 633 (Invitrogen).

Parasites. Cysts of the avirulent ME-49 strain of *T. gondii* were obtained from the brains of chronically infected C57BL/6 mice. For experimental infection, animals received 20 cysts i.p. in 0.5 ml PBS. The transgenic parasites p30-OVA (TgOVA) (15), p30-OVA-YFP-YFP (TgOVAYFP), and p30-RFP (TgRFP; provided by B. Striepen and M.-J. Gubbels, University of Georgia, Athens, GA) (16), and the nontransgenic RH strains of *T. gondii* were maintained by serial passage on human foreskin fibroblasts (HFFs) cultured at 37°C in DMEM (Invitrogen) supplemented with 10% heat-inactivated FBS. Parasites were harvested from 80% lysed HFF monolayers. Soluble tachyzoite Ag (STAg) was prepared as previously described (47). Where indicated in the figures, parasites received the following treatments: HK parasites were incubated at 56°C for 20 min; live nonmultiplying tachyzoites (irr) were obtained by irradiation with 15,000 rads (Mark I cesium irradiator; J.L. Shepherd); fixed parasites (fix) were incubated with 4% paraformaldehyde (PFA) for 10 min at room temperature (RT) and extensively washed with PBS; and for antibody opsonization, tachyzoites were incubated with immune sera from chronically infected mice for 30 min at 4°C followed by washing with PBS. For the mixed parasite cultures, HK and irr tachyzoites were mixed at a 1:1 ratio and added to DC cultures. For Western blotting, 5×10^6 tachyzoites were lysed in cell lysis buffer (Cell Signaling Technology) and analyzed by SDS-PAGE. Western blotting was performed using a rabbit anti-OVA antibody (1:10,000) or rabbit anti-SAG1 (1:10,000), followed with anti–rabbit Ig–horseradish peroxidase (1:3,000; GE Healthcare).

Generation of Ag-presenting cells. BMDCs from C57BL/6 mice were obtained as previously described (48) and incubated with treated or untreated *T. gondii* tachyzoites at a ratio of 1–4 parasites/DC. The cells were then incubated for different time periods (3.5–18 h), free-floating parasites were removed by extensive washing (centrifugation performed at 900 rpm for 10 min), and DCs were used for T cell activation assays or analyzed by flow cytometry. Where indicated in the figures, ExoA was added to the cultures at a final concentration of 10 μg/ml. For T cell priming assays, DCs were fixed with 0.001% glutaraldehyde for 30 s, the reaction was stopped with 0.2 M PBS/glycine, and the cells were washed with RPMI 1640 supplemented with 10% FCS. Before fixation, cell samples were prepared in a cytospin and stained using Diff Quick (Dade Behring) to evaluate the level of infection.

In some experiments, splenic DCs derived from C57BL/6 or MHC-$I^{-/-}$ animals were substituted for BMDCs. Spleens were digested with 400 μg/ml Liberase CI solution (Roche) in RPMI 1640 for 30 min at 37°C and were homogenized into single-cell suspensions. DCs were purified by positive selection using anti-CD11c MACS beads (Miltenyi Biotec) according to the manufacturer's protocol. The purity of $CD11c^+$ cells was 70–85%, as determined by flow cytometry. Purified $CD11c^+$ cells were then exposed to *T. gondii* tachyzoites as described.

To inhibit the parasite invasion process, live tachyzoites were treated with increasing concentrations of 4-p-BPB or DMSO vehicle alone for 10 min at 37°C and, after extensive washing, were added to DC cultures. Where indicated in the figures, 4-p-BPB–pretreated parasites were opsonized as described in the previous section before co-culture with DCs.

In a different set of experiments, parasites were incubated with 10 μM CytD or DMSO control for 10 min at RT and for an additional 30 min with DCs in the presence of the drug. DCs were washed to eliminate both the extracellular parasites and the drug, and were incubated for 3.5 h to allow for Ag processing and presentation before fixation. In the same experiments, DCs were incubated with CytD for the same time period, and after washing, 1 mg/ml of soluble OVA was added to the cultures.

For experiments using Ag-coated latex beads (3 μm; Sigma-Aldrich), 10^8 beads were incubated overnight on agitation at 4°C with 1 mg/ml of soluble OVA. The beads were extensively washed with PBS and added to DCs at 10:1 ratio either alone or together with *T. gondii* tachyzoites, as indicated in the figures. Where mentioned, DCs were pulsed with control peptides, 0.1 nM $OVA_{(257–264)}$ (SIINFEKL), and 1 μM $OVA_{(323–339)}$ for MHC class I and II, respectively.

Purification, CFSE labeling, and in vitro activation of $CD8^+$ OT-I and $CD4^+$ OT-II cells. Spleens and lymph nodes were mechanically disrupted and red blood cells were removed by lysis with ACK Lysing Buffer (Cambrex Bio Science). $CD8^+$ and $CD4^+$ lymphocytes were purified by negative selection using MACS microbeads (Miltenyi Biotec) according to the manufacturer's protocol. The purity of the T cell populations was >95%, as determined by flow cytometry. Where indicated in the figures,

purified lymphocytes were labeled with the intracellular fluorescent dye CFSE (Invitrogen). The cells were incubated at 10^7 cells/ml in PBS with 1 μM CFSE for 10 min at 37°C, the reaction was stopped with 10% normal mouse serum, and the cells were washed twice with RPMI 1640 supplemented with 10% FCS. CFSE-labeled T cells were plated at 10^6 cells/well in 24-well plates, and parasite-exposed DCs were added at a 3:1 T cell/DC ratio. T cell proliferation was measured 72 h later as the percentage of cells showing reduced CFSE content within the $CD4^+$ or $CD8^+$ T cell population using a FACSCalibur (BD), and data were analyzed with FlowJo software (Tree Star, Inc.).

Adoptive transfer and in vivo activation of OT-I T cells. Purified OT-I cells were labeled with 5 μM CFSE, as described in the previous section, and $3–5 \times 10^6$ cells were injected i.v. into B6.SJL congenic recipients on day −1. Mice were challenged by s.c. injection of $0.5–10^6$ tachyzoites or 2×10^5 MHC-$I^{-/-}$–infected splenic $CD11c^+$ cells. Draining lymph nodes were harvested 3 d later and T cell proliferation was analyzed by flow cytometry. Transferred $CD8^+$ OT-I T cells were gated based on CD45.2, CD3, and CD8 surface marker expression.

Measurement of thymidine incorporation and IFN-γ production by T lymphocytes. 10^5 purified OT-I T cells were co-cultured with 5×10^4 parasite-exposed DCs in 96-well, round-bottom microtiter plates, and the culture supernatants were harvested at 48 h for cytokine measurement by ELISA. The cells were pulsed with 1 μCi [^{3}H]thymidine per well (New England Nuclear) for an additional 18 h, and the incorporated radioactivity was measured (1450 MicroBeta TriLux; PerkinElmer).

In a different set of experiments, $CD8^+$ T lymphocytes obtained from day 7 *T. gondii*–infected mice ($n = 3$ per group) were used as the responding cell population. Spleens were mechanically disrupted and red blood cells were removed by lysis with ACK lysing buffer (Cambrex Bio Science). $CD8^+$ T lymphocytes were purified by negative selection and incubated with parasite-exposed DCs as described or where indicated in the figures, with DCs preexposed to 10 μg/ml STAg.

Immunofluorescence, immunocytochemistry, and transmission electron microscopy (TEM). For immunofluorescence, DCs were plated on polylysine-treated coverslips (BD) and infected with live *T. gondii* tachyzoites at a multiplicity of infection (MOI) of 1 for 12 h. Cells were fixed with 4% PFA for 10 min and washed three to four times with PBS before permeabilization with 0.2% saponin for 15 min and blocking with PBS/3% BSA/0.1% saponin for 1 h. Cells were incubated with the primary antibody for 1 h and washed four times before the secondary antibody was added for a similar time period. After extensive washing, coverslips were mounted using antifade mounting solution (ProLong Gold; Invitrogen). All incubations were performed at RT. Images were acquired using a confocal microscope (model SP5; Leica) using a 63× oil immersion objective NA1.4. Huygens Essential (version 3.3; Scientific Volume Imaging BV) and Imaris (version 6.1.5; Bitplane AG) software were used for deconvolution and colocalization analyses.

For immuno-EM, parasite-exposed DCs were fixed with 4% PFA in 0.25 M Hepes (pH 7.4) for 1 h at RT, followed by 8% PFA in the same buffer overnight at 4°C. Cryosectioning and immunolabeling was performed as previously described (49). G6Pase activity was revealed by cytochemistry as previously described (50), and quantification of G6Pase-positive compartments was performed in a single EM plane.

Vaccinia virus infections. DCs were infected with rVV-OVA (51) at an MOI of 10 for 20 min at 37°C, with mixing every few minutes in balanced salt solution containing 0.1% BSA. Cells were incubated at 37°C in growth media for the remainder of the assay in the presence or absence of 10 μg/ml ExoA. Samples were taken at different time points after infection, and the generation of K^b–SIINFEKL complexes was analyzed by flow cytometry with 25D1.16–Alexa Fluor 647 mAb on an LSR II (BD) using FACSDiva software (BD), and data were analyzed using FlowJo software. Alternatively, infected DCs were fixed and used for T cell activation assays.

Statistics. The statistical significance of differences in the means of experimental groups was determined using an unpaired, two-tailed Student's *t* test.

Online supplemental material. Fig. S1 shows that transgenic parasites secrete OVA via the default secretory pathway. Fig. S2 demonstrates the ability of infected WT DCs to induce OT-I cell proliferation in vivo. Fig. S3 shows that splenic-derived DCs are unable to cross-present parasite-derived Ag from phagocytosed tachyzoites. Fig. S4 demonstrates that infected DCs can also phagocytose dead parasites, and that in mixed cultures the majority of DCs phagocytose both latex beads and dead tachyzoites. Fig. S5 shows that targeting of either live or dead parasites to FcγR fails to result in MHC class I cross-presentation and that OVA production is not affected in antibody-opsonized or 4-p-BPB–treated parasites. Fig. S6 shows lysosome fusion with parasite-containing phagosome but not with PV. Fig. S7 provides controls for possible nonspecific effects of ExoA treatment on endogenous class I presentation, MHC-I surface expression, parasite infectivity, and parasite protein production. Online supplemental material is available at http://www.jem.org/cgi/content/full/jem.20082108/DC1.

The authors thank S. Hieny and S. White for their expert technical assistance. We are also indebted to the members of the Biological Imaging Facility (Research Technologies Branch, NIAID), particularly J. Kabat, for their expert support in confocal microscopy. In addition, we are grateful to D. Jankovic, S. Bertholet, and J. Romano for their input in different aspects of this project, and to B. Striepen and M.-J. Gubbels for providing the fluorochrome transgenic parasites. Finally, we thank D. Sacks, J. Yewdell, J. Bennink, J. Boothroyd, and M. Desjardins for their invaluable advice and discussion.

This research was supported by the Intramural Research Program of the NIAID. The authors have no conflicting financial interests.

Submitted: 22 September 2008
Accepted: 26 December 2008

REFERENCES

1. Mellman, I., and R.M. Steinman. 2001. Dendritic cells: specialized and regulated antigen processing machines. *Cell*. 106:255–258.
2. Trombetta, E.S., and I. Mellman. 2005. Cell biology of antigen processing in vitro and in vivo. *Annu. Rev. Immunol.* 23:975–1028.
3. Burgdorf, S., C. Scholz, A. Kautz, R. Tampe, and C. Kurts. 2008. Spatial and mechanistic separation of cross-presentation and endogenous antigen presentation. *Nat. Immunol.* 9:558–566.
4. Carruthers, V.B., and L.D. Sibley. 1997. Sequential protein secretion from three distinct organelles of *Toxoplasma gondii* accompanies invasion of human fibroblasts. *Eur. J. Cell Biol.* 73:114–123.
5. Mordue, D.G., S. Hakansson, I. Niesman, and L.D. Sibley. 1999. *Toxoplasma gondii* resides in a vacuole that avoids fusion with host cell endocytic and exocytic vesicular trafficking pathways. *Exp. Parasitol.* 92:87–99.
6. Gazzinelli, R.T., F.T. Hakim, S. Hieny, G.M. Shearer, and A. Sher. 1991. Synergistic role of CD4+ and CD8+ T lymphocytes in IFN-gamma production and protective immunity induced by an attenuated *Toxoplasma gondii* vaccine. *J. Immunol.* 146:286–292.
7. Suzuki, Y., and J.S. Remington. 1988. Dual regulation of resistance against *Toxoplasma gondii* infection by Lyt-2+ and Lyt-1+, L3T4+ T cells in mice. *J. Immunol.* 140:3943–3946.
8. Mordue, D.G., and L.D. Sibley. 1997. Intracellular fate of vacuoles containing *Toxoplasma gondii* is determined at the time of formation and depends on the mechanism of entry. *J. Immunol.* 159:4452–4459.
9. Joiner, K.A., S.A. Fuhrman, H.M. Miettinen, L.H. Kasper, and I. Mellman. 1990. *Toxoplasma gondii*: fusion competence of parasitophorous vacuoles in Fc receptor-transfected fibroblasts. *Science*. 249:641–646.
10. Schwab, J.C., C.J. Beckers, and K.A. Joiner. 1994. The parasitophorous vacuole membrane surrounding intracellular *Toxoplasma gondii* functions as a molecular sieve. *Proc. Natl. Acad. Sci. USA*. 91:509–513.

11. Sinai, A.P., P. Webster, and K.A. Joiner. 1997. Association of host cell endoplasmic reticulum and mitochondria with the *Toxoplasma gondii* parasitophorous vacuole membrane: a high affinity interaction. *J. Cell Sci.* 110:2117–2128.
12. Gupta, N., M.M. Zahn, I. Coppens, K.A. Joiner, and D.R. Voelker. 2005. Selective disruption of phosphatidylcholine metabolism of the intracellular parasite *Toxoplasma gondii* arrests its growth. *J. Biol. Chem.* 280:16345–16353.
13. Crawford, M.J., N. Thomsen-Zieger, M. Ray, J. Schachtner, D.S. Roos, and F. Seeber. 2006. *Toxoplasma gondii* scavenges host-derived lipoic acid despite its de novo synthesis in the apicoplast. *EMBO J.* 25:3214–3222.
14. Coppens, I., J.D. Dunn, J.D. Romano, M. Pypaert, H. Zhang, J.C. Boothroyd, and K.A. Joiner. 2006. *Toxoplasma gondii* sequesters lysosomes from mammalian hosts in the vacuolar space. *Cell.* 125:261–274.
15. Bertholet, S., R. Goldszmid, A. Morrot, A. Debrabant, F. Afrin, C. Collazo-Custodio, M. Houde, M. Desjardins, A. Sher, and D. Sacks. 2006. *Leishmania* antigens are presented to CD8+ T cells by a transporter associated with antigen processing-independent pathway in vitro and in vivo. *J. Immunol.* 177:3525–3533.
16. Gubbels, M.J., B. Striepen, N. Shastri, M. Turkoz, and E.A. Robey. 2005. Class I major histocompatibility complex presentation of antigens that escape from the parasitophorous vacuole of *Toxoplasma gondii*. *Infect. Immun.* 73:703–711.
17. Goldszmid, R.S., A. Bafica, D. Jankovic, C.G. Feng, P. Caspar, R. Winkler-Pickett, G. Trinchieri, and A. Sher. 2007. TAP-1 indirectly regulates $CD4^+$ T cell priming in *Toxoplasma gondii* infection by controlling NK cell IFN-γ production. *J. Exp. Med.* 204:2591–2602.
18. Dzierszinski, F., M. Pepper, J.S. Stumhofer, D.F. LaRosa, E.H. Wilson, L.A. Turka, S.K. Halonen, C.A. Hunter, and D.S. Roos. 2007. Presentation of *Toxoplasma gondii* antigens via the endogenous major histocompatibility complex class I pathway in nonprofessional and professional antigen-presenting cells. *Infect. Immun.* 75:5200–5209.
19. Saffer, L.D., S.A. Long Krug, and J.D. Schwartzman. 1989. The role of phospholipase in host cell penetration by *Toxoplasma gondii*. *Am. J. Trop. Med. Hyg.* 40:145–149.
20. Hakansson, S., A.J. Charron, and L.D. Sibley. 2001. *Toxoplasma* evacuoles: a two-step process of secretion and fusion forms the parasitophorous vacuole. *EMBO J.* 20:3132–3144.
21. Boothroyd, J.C., and J.F. Dubremetz. 2008. Kiss and spit: the dual roles of *Toxoplasma* rhoptries. *Nat. Rev. Microbiol.* 6:79–88.
22. Regnault, A., D. Lankar, V. Lacabanne, A. Rodriguez, C. Thery, M. Rescigno, T. Saito, S. Verbeek, C. Bonnerot, P. Ricciardi-Castagnoli, and S. Amigorena. 1999. Fcγ receptor–mediated induction of dendritic cell maturation and major histocompatibility complex class I–restricted antigen presentation after immune complex internalization. *J. Exp. Med.* 189:371–380.
23. Houde, M., S. Bertholet, E. Gagnon, S. Brunet, G. Goyette, A. Laplante, M.F. Princiotta, P. Thibault, D. Sacks, and M. Desjardins. 2003. Phagosomes are competent organelles for antigen cross-presentation. *Nature.* 425:402–406.
24. Guermonprez, P., L. Saveanu, M. Kleijmeer, J. Davoust, P. Van Endert, and S. Amigorena. 2003. ER-phagosome fusion defines an MHC class I cross-presentation compartment in dendritic cells. *Nature.* 425:397–402.
25. Ackerman, A.L., C. Kyritsis, R. Tampe, and P. Cresswell. 2003. Early phagosomes in dendritic cells form a cellular compartment sufficient for cross presentation of exogenous antigens. *Proc. Natl. Acad. Sci. USA.* 100:12889–12894.
26. Martin, A.M., T. Liu, B.C. Lynn, and A.P. Sinai. 2007. The *Toxoplasma gondii* parasitophorous vacuole membrane: transactions across the border. *J. Eukaryot. Microbiol.* 54:25–28.
27. Gajria, B., A. Bahl, J. Brestelli, J. Dommer, S. Fischer, X. Gao, M. Heiges, J. Iodice, J.C. Kissinger, A.J. Mackey, et al. 2008. ToxoDB: an integrated *Toxoplasma gondii* database resource. *Nucleic Acids Res.* 36:D553–D556.
28. Ajioka, J.W., A. Soldati, and D. Soldati. 2007. Toxoplasma: Molecular and Cellular Biology. Horizon Scientific Press, Hethersett, England, UK. 202 pp.
29. Koopmann, J.O., J. Albring, E. Huter, N. Bulbuc, P. Spee, J. Neefjes, G.J. Hammerling, and F. Momburg. 2000. Export of antigenic peptides from the endoplasmic reticulum intersects with retrograde protein translocation through the Sec61p channel. *Immunity.* 13:117–127.
30. Woodworth, J.S., and S.M. Behar. 2006. *Mycobacterium tuberculosis*-specific CD8+ T cells and their role in immunity. *Crit. Rev. Immunol.* 26:317–352.
31. Hafalla, J.C., U. Rai, D. Bernal-Rubio, A. Rodriguez, and F. Zavala. 2007. Efficient development of plasmodium liver stage-specific memory CD8+ T cells during the course of blood-stage malarial infection. *J. Infect. Dis.* 196:1827–1835.
32. Belkaid, Y., E. Von Stebut, S. Mendez, R. Lira, E. Caler, S. Bertholet, M.C. Udey, and D. Sacks. 2002. CD8+ T cells are required for primary immunity in C57BL/6 mice following low-dose, intradermal challenge with *Leishmania major*. *J. Immunol.* 168:3992–4000.
33. Ackerman, A.L., A. Giodini, and P. Cresswell. 2006. A role for the endoplasmic reticulum protein retrotranslocation machinery during crosspresentation by dendritic cells. *Immunity.* 25:607–617.
34. Touret, N., P. Paroutis, M. Terebiznik, R.E. Harrison, S. Trombetta, M. Pypaert, A. Chow, A. Jiang, J. Shaw, C. Yip, et al. 2005. Quantitative and dynamic assessment of the contribution of the ER to phagosome formation. *Cell.* 123:157–170.
35. Desjardins, M. 1995. Biogenesis of phagolysosomes: the 'kiss and run' hypothesis. *Trends Cell Biol.* 5:183–186.
36. Rusinol, A.E., Z. Cui, M.H. Chen, and J.E. Vance. 1994. A unique mitochondria-associated membrane fraction from rat liver has a high capacity for lipid synthesis and contains pre-Golgi secretory proteins including nascent lipoproteins. *J. Biol. Chem.* 269:27494–27502.
37. Vance, J.E. 1990. Phospholipid synthesis in a membrane fraction associated with mitochondria. *J. Biol. Chem.* 265:7248–7256.
38. Saeij, J.P., S. Coller, J.P. Boyle, M.E. Jerome, M.W. White, and J.C. Boothroyd. 2007. *Toxoplasma* co-opts host gene expression by injection of a polymorphic kinase homologue. *Nature.* 445:324–327.
39. Saeij, J.P., J.P. Boyle, S. Coller, S. Taylor, L.D. Sibley, E.T. Brooke-Powell, J.W. Ajioka, and J.C. Boothroyd. 2006. Polymorphic secreted kinases are key virulence factors in toxoplasmosis. *Science.* 314:1780–1783.
40. Taylor, S., A. Barragan, C. Su, B. Fux, S.J. Fentress, K. Tang, W.L. Beatty, H.E. Hajj, M. Jerome, M.S. Behnke, et al. 2006. A secreted serine-threonine kinase determines virulence in the eukaryotic pathogen *Toxoplasma gondii*. *Science.* 314:1776–1780.
41. Andrade, R.M., M. Wessendarp, M.J. Gubbels, B. Striepen, and C.S. Subauste. 2006. CD40 induces macrophage anti-*Toxoplasma gondii* activity by triggering autophagy-dependent fusion of pathogen-containing vacuoles and lysosomes. *J. Clin. Invest.* 116:2366–2377.
42. Zhao, Y., D. Wilson, S. Matthews, and G.S. Yap. 2007. Rapid elimination of *Toxoplasma gondii* by gamma interferon-primed mouse macrophages is independent of CD40 signaling. *Infect. Immun.* 75:4799–4803.
43. Ling, Y.M., M.H. Shaw, C. Ayala, I. Coppens, G.A. Taylor, D.J. Ferguson, and G.S. Yap. 2006. Vacuolar and plasma membrane stripping and autophagic elimination of *Toxoplasma gondii* in primed effector macrophages. *J. Exp. Med.* 203:2063–2071.
44. Blanchard, N., F. Gonzalez, M. Schaeffer, N.T. Joncker, T. Cheng, A.J. Shastri, E.A. Robey, and N. Shastri. 2008. Immunodominant, protective response to the parasite *Toxoplasma gondii* requires antigen processing in the endoplasmic reticulum. *Nat. Immunol.* 9:937–944.
45. Frickel, E.M., N. Sahoo, J. Hopp, M.J. Gubbels, M.P. Craver, L.J. Knoll, H.L. Ploegh, and G.M. Grotenbreg. 2008. Parasite stage-specific recognition of endogenous *Toxoplasma gondii*-derived CD8+ T cell epitopes. *J. Infect. Dis.* 198:1579–1581.
46. Porgador, A., J.W. Yewdell, Y. Deng, J.R. Bennink, and R.N. Germain. 1997. Localization, quantitation, and in situ detection of specific peptide-MHC class I complexes using a monoclonal antibody. *Immunity.* 6:715–726.
47. Grunvald, E., M. Chiaramonte, S. Hieny, M. Wysocka, G. Trinchieri, S.N. Vogel, R.T. Gazzinelli, and A. Sher. 1996. Biochemical characterization and protein kinase C dependency of monokine-inducing activities of *Toxoplasma gondii*. *Infect. Immun.* 64:2010–2018.

48. Goldszmid, R.S., J. Idoyaga, A.I. Bravo, R. Steinman, J. Mordoh, and R. Wainstok. 2003. Dendritic cells charged with apoptotic tumor cells induce long-lived protective CD4+ and CD8+ T cell immunity against B16 melanoma. *J. Immunol.* 171:5940–5947.
49. Quittnat, F., Y. Nishikawa, T.T. Stedman, D.R. Voelker, J.Y. Choi, M.M. Zahn, R.C. Murphy, R.M. Barkley, M. Pypaert, K.A. Joiner, and I. Coppens. 2004. On the biogenesis of lipid bodies in ancient eukaryotes: synthesis of triacylglycerols by a *Toxoplasma* DGAT1-related enzyme. *Mol. Biochem. Parasitol.* 138:107–122.
50. Griffiths, G., P. Quinn, and G. Warren. 1983. Dissection of the Golgi complex. I. Monensin inhibits the transport of viral membrane proteins from medial to trans Golgi cisternae in baby hamster kidney cells infected with Semliki Forest virus. *J. Cell Biol.* 96: 835–850.
51. Princiotta, M.F., D. Finzi, S.B. Qian, J. Gibbs, S. Schuchmann, F. Buttgereit, J.R. Bennink, and J.W. Yewdell. 2003. Quantitating protein synthesis, degradation, and endogenous antigen processing. *Immunity.* 18:343–354.